AIAA 80-0124R

Dryden Lectureship in Research

Flow in Transonic Compressors

Jack L. Kerrebrock
Massachusetts Institute of Technology, Cambridge, Mass.

Introduction

By the term transonic compressor we mean an axial flow compressor in which the inlet flow Mach number, relative to the rotating blades, varies from below unity at radii near the inner casing or hub to values substantially above unity at radii near the blade tips. Usually the flow is diffused to subsonic velocities in the flow passages formed by the rotating blades, generating part of the desired pressure rise. A further pressure rise is generated in a stationary blade row downstream of the rotor in the process of removing the swirl imparted by the rotor, but the flow Mach numbers relative to the stator blades are generally below unity. Thus, the flows of principle concern here are those in the rotor passages.

Axial flow compressors have been the subject of research and development efforts for at least 40 years, and the transonic compressor for nearly 30. The earliest systematic studies in the United States were carried out by the Lewis Research Center of the NACA about 1950, and the technology was quickly developed for application in the first generation of turbofan engines.[1] Because it offers higher pressure ratios per stage and larger airflows per unit of engine frontal area than the subsonic compressor, the transonic compressor has become a major component of all modern aircraft engines. It has received a proportionately large share of the huge research and development effort expended on these engines. The opinion has often been proffered that it represents a highly developed technology which will not yield significant gains from additional research and development.

I argue to the contrary, that there is much scope for improvement in the design of these important components, and that the capability for making these improvements is rapidly coming to hand. This position rests on several facts. First, there are large inefficiencies in transonic compressors due to the three-dimensional character of the inviscid and viscous flows and their coupling. Second, the design methods currently in use do not deal rationally with these loss mechanisms. Third, until recently there has not been a capability for measuring the actual flow in the rotor passages to provide feedback to the design process. The designer has had to rely on overall performance measurements and time-averaged measurements between the blade rows for verification of the design process. We now have several diagnostic methods capable of providing detailed information about the flow in the blade passages. These include laser velocimetry, gas fluorescent density measurements, and time-resolved pressure measurements, as well as the time-honored hot-wire anemometer. We also have a capability for numerical computation of the three-dimensional transonic flow, inviscid at present but with viscous effects in the near future. Turbomachinery should be one of the major beneficiaries of the advances in this area as was discussed by Chapman in last year's Dryden Lecture.[2] Taken together, the problem of the transonic compressor and these new engineering tools represent an opportunity quite comparable to that presented by recent improvements in high-speed airfoil sections, together with three-dimensional computational techniques in external aerodynamics.

My objectives in this paper are to describe the role of the technology and its status, discusss some recent progress toward understanding the flowfield, and indicate the directions which I feel future work should take. I do so with the full knowledge that some of my colleagues in industry and government have much more experience in the design of compressors than I, and that I may not fully represent their viewpoint. My hope is that the view expressed here will prove complementary to that of practicing engineers, and have some beneficial effect on future fan and compressor designs.

This review will deal mainly with the question of efficiency. There are many other important problems in the design of transonic compressors, including flutter and forced vibration, stall and surge, foreign object damage, and noise. Some will be mentioned as they impinge on the issue of design for high efficiency, but only the latter will be discussed in detail. Apart from the necessity for focusing on one of these many issues in order to achieve the depth appropriate to a Research Lecture, this choice is motivated by the perception that efficiency is the

Professor Kerrebrock is Richard Cockburn Maclaurin Professor and Head of the Department of Aeronautics and Astronautics at the Massachusetts Institute of Technology. He has taught and conducted research in energy conversion and propulsion since 1956 when he received his Ph.D. degree from the California Institute of Technology. His early work was on nuclear rockets, space propulsion and power, and magnetohydrodynamic generators. More recently, he has addressed the fluid mechanics of turbomachinery for aircraft engines, and is the author of a text on aircraft engines and gas turbines. He was the Director of the MIT Gas Turbine Laboratory from 1968 to 1978. Professor Kerrebrock is a Fellow of the AIAA, a member of the National Academy of Engineering, the Air Force Scientific Advisory Board, the Aeronautics and Space Engineering Board of the NRC, and the Aeronautics Advisory Committee of NASA.

Presented as Paper 80-0124 at the AIAA 18th Aerospace Sciences Meeting, Pasadena, Calif., Jan. 14-16, 1980; submitted Feb. 6, 1980; revision received Sept. 11, 1980.

most sensitive indicator of the quality of the aerodynamic design of the compressor.

Since this Lecture is aimed at a general audience, it will be necessary to restate some concepts and facts which are second nature to experts in turbomachinery, while omitting details of urgent importance to them, and at the same time present some results without adequate explanation for the general reader. I hope both groups will be tolerant of the compromise I have selected.

Role of the Technology

To minimize the weight and drag of an aircraft engine, it is desirable to have as large a mass flow per unit of frontal area as possible, particularly in the first stage of the compressor. This drives the design toward high axial flow Mach numbers and toward small ratios of hub radius to tip radius. The pressure ratio available per stage rises rapidly with increasing blade tangential Mach number, as may be seen from the Euler turbine equation which states that the stagnation enthalpy rise across a rotor $H_2 - H_1$ is given by the product of the angular velocity of the rotor ω and the change in angular momentum per unit mass which the fluid experiences in passing through the rotor, $v_2 r_2 - v_1 r_1$, where v is the absolute tangential velocity and r is the streamtube radius. Thus $H_2 - H_1 = \omega(v_2 r_2 - v_1 r_1)$ and if we represent H by $c_p T_t$ where T_t is the stagnation temperature and assume isentropic flow so that $P_2/P_1 = (T_2/T_1)^{\gamma/\gamma-1}$ we find

$$\left(\frac{P_{t2}}{P_{t1}}\right)^{\frac{\gamma-1}{\gamma}} = 1 + \frac{(\gamma-1)M_T^2}{1+\frac{\gamma-1}{2}M_1^2}\left(\frac{r_2}{r_1}\frac{v_2}{\omega r_1} - \frac{v_1}{\omega r_1}\right) \qquad (1)$$

where $M_T^2 = (\omega r_1)^2/RT_1$ is the square of the tangential Mach number of the rotor blade at the upstream radius of the stream tube r_1 and M_1 is the upstream flow Mach number. If we assume for the moment that the quantity in parentheses is controlled by the geometry of a rotor and is not very sensitive to its angular velocity, we see that the stage temperature rise increases roughly as the square of M_T, with a corresponding variation of pressure ratio.

Until the development of high-strength titanium alloys, blade centrifugal and vibrational stresses placed serious limits on the tip speeds of blading, especially for low hub-to-tip radius ratios. It is now possible to design rotors for operation at tip speeds of more than 550 m/s, which yields $M_T = 1.7$ at the tip for an axial Mach number $M_1 = 0.7$ at standard temperature.

The front fan in a turbofan engine such as that shown in cutaway in Fig. 1 provides a combination of motivations for operation transonically. To minimize noise a single stage is desirable, and cycle considerations dictate a pressure ratio of about 1.6. This is difficult to achieve with M_T less than about 1.2. The fan is driven by a low-pressure turbine, which is one of the heavier and more expensive components of the engine. This turbine is subject to the same Euler equation (1) as the compressor, so to develop high power per stage it too should have as high a tangential Mach number as possible. Because it operates in hot gas, this implies as high a tangential velocity as is practical. Since the fan and turbine are usually directly coupled and the fan has a large diameter, its tip Mach number is driven up by the turbine requirements. Finally, improvements in materials and cooling technology have enabled the use of higher turbine inlet temperature, which in turn permits higher bypass ratios, emphasizing the geometrical effects just described.

The combination of opportunities and constraints thus far outlined has no aerodynamic content. The compressor designer is faced with the problem of contriving a blade configuration which will operate stably and with high efficiency, while meeting this set of requirements.

There is a powerful incentive to achieve high efficiency. For an engine flying at 0.8 Mach number and having characteristics typical of current high-bypass engines, fuel flow decreases 0.7% for each 1.0% increase in fan efficiency. Improvements in the efficiency of the compressor, high-pressure turbine, and low-pressure turbine will yield comparable reductions in fuel consumption.

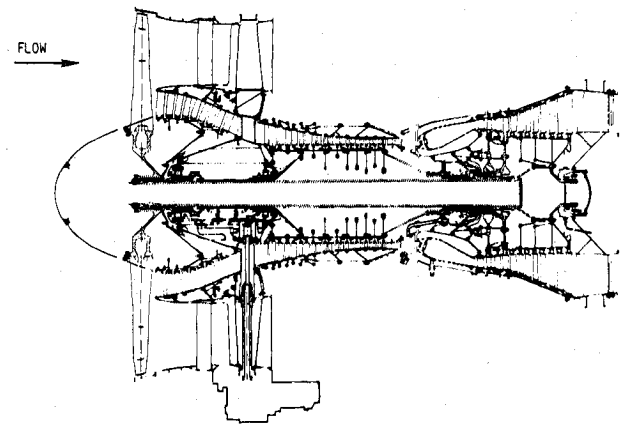

Fig. 1 Cutaway of modern high bypass turbofan engine (Pratt & Whitney JT9D).

Performance of Existing Rotors

To establish a basis for detailed discussion of the flowfield we begin by assessing the performance of existing rotors, as measured by pressure rise and efficiency. In fact, as noted above, the emphasis will be on efficiency because it is the more sensitive indicator of quality of the rotor design. By empirical iteration it is usually possible to arrive at choices for blade shape and spacing which give the peripherally averaged rotor exit flow angles and velocities required for the desired pressure ratio. There is some uncertainty due to the effects of suction surface separation on the exit flow angle (deviation) and of losses on the mean flowfield, but these can be compensated for empirically. Thus a highly developed rotor will meet its weight flow and pressure ratio specifications, although the process of bringing it to this state is likely to be long and expensive.

But how does its efficiency compare with expectations, and what are reasonable expectations? This last question is a difficult one. We take the position here that for the portion of the flow away from the end walls the losses in a rotor in principle need not be larger than the sum of those due to profile drag on the blades as found from cascade tests of the airfoil sections, plus those due to stagnation pressure loss across the shock system implied by the conceptual design of the rotor.

All transonic compressors in use are of the shock-in-rotor type in which the flow is decelerated within the rotor passages by a shock system, the rotor exit relative velocity usually but not always being less than sonic. The absolute velocity at the rotor exit is subsonic in all cases, however, so the stators are subsonic.

A typical cascade geometry is indicated in Fig. 2, with the notation which will be used to describe it. The relative Mach number M_1' dictates the blade design to a large extent in conventional schemes. In the design shown, the suction surface of the blade is flat and aligned to the inflow far upstream. The passage shock may be nearly normal or oblique, depending on the magnitude of M_1' and the rotor pressure ratio. It seems clear that in an efficient design the pressure ratio across the passage shock should not be larger than the static pressure ratio across the rotor. An upper limit would seem to be the stage pressure ratio. Thus for this type of rotor we take the expected shock loss to be that across an oblique shock having the pressure ratio of the stage. The maximum shock loss which would be expected to occur, unless the flow

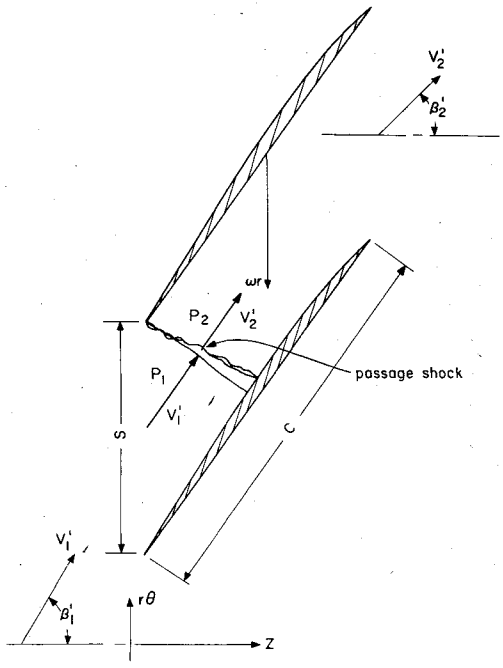

Fig. 2 Typical supersonic cascade geometry, with fan entrance flow aligned to nearly flat suction surface.

is overaccelerated in the rotor, is that for a normal shock at the relative Mach number M_1', so this will be taken as an upper limit on shock losses.

Establishing a reasonable level for viscous losses is more difficult. It is common practice to use the "D factor" correlation of Leiblein[3] to relate the stagnation pressure loss across the cascade to the inlet and exit velocities and the solidity $\sigma = c/s$. Since its derivation from low-speed cascade data, this correlation has been modified to account for radial variations in losses and for differences between subsonic and transonic cascades.[4] These latter modifications really represent attempts to include the effects of three-dimensional flow in the cascade loss correlation, and in this sense are configuration specific. We, therefore, take the position that the original Leiblein correlation represents a reasonable estimate of profile losses, as distinct from the losses which result from three-dimensional effects and from interaction between the shocks and boundary layers.

The D factor is defined as

$$D = 1 - \frac{V_2'}{V_1'} + \frac{v_2 - v_1}{2\sigma V_1'} \tag{2}$$

and the loss factor by

$$\bar{\omega}_1' = \frac{\overline{P_{t2}'} - P_{t1}'}{P_{t1}' - P_1} \tag{3}$$

where P_t' is the stagnation pressure relative to the rotor and the overbar indicates a peripheral average over the outflow. The correlation is of the form,

$$\frac{\omega_1' \cos^3 \beta_2'}{2\sigma \cos^2 \beta_1'} = \Omega(D) \tag{4}$$

For the present purposes it will be represented by $\Omega(D) = 0.005 + 0.160\, D^4$, which fits the data of Ref. 3 rather well.

It is readily demonstrated that for given V_1', V_2', β_1', and β_2' there is a value of σ which minimizes $\bar{\omega}_1$ or, alternatively, a value of D which minimizes $\bar{\omega}_1$ for given V_2'/V_1'. This relationship is shown in Fig. 3. Design values for an assortment of rotors to be discussed below are indicated for comparison. The symbols are identified in Table 1. The normal range of V_2'/V_1' is about 0.8-0.5, and the corresponding range of D is 0.4-0.6. Thus Ω will not exceed about 0.025. It is important to note, however, that for this (optimum) level of Ω, the loss factor $\bar{\omega}_1'$ increases with both solidity σ and the exit flow angle β_2'.

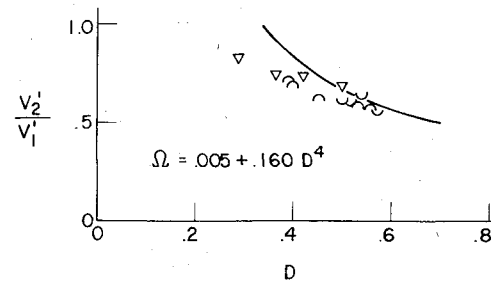

Fig. 3 D factor which minimizes cascade loss as function of exit-to-inlet relative velocity ratio (data points are from rotors identified in

Efficiency estimates based on these assumptions for shock and viscous losses are given as functions of tangential Mach number in Fig. 4 for rotors having stagnation pressure ratios of 1.6 and 2.0. For each pressure ratio, two cases are shown, one with an oblique passage shock having a pressure ratio equal to the stage pressure ratio, and one with a normal shock at the relative Mach number M_1'. We note that with oblique shocks the efficiencies are high indeed, better than 0.95 at Mach numbers as high as 2.0. With normal shock losses they naturally are much lower at the high Mach number.

Plotted on this figure are measured streamline efficiencies* for a sizeable number of transonic rotors, some with excellent overall efficiency and some rather poor in this regard. The data plotted are only for the portions of each rotor for which $M_1' > 1$; some have extensive regions of subsonic flow at smaller radii which contribute to their good overall efficiency.

Two observations follow from Fig. 4. First, in most cases the actual streamline efficiencies are well below the lowest estimate based on normal shock losses. Second, the dominant trend is a reduction of efficiency with increasing radius, not solely with increasing Mach number. In fact, for a given tangential Mach number there is a systematic trend of increasing efficiency with increasing tip Mach number.

The geometrical trend is shown more clearly in Fig. 5 where some of the data of Fig. 4 have been replotted on an abscissa which is the ratio of the radius of the streamline at the exit from the rotor to the tip radius there. The several sets of data have tip tangential Mach numbers ranging 1.29-1.65, yet most display roughly the same trend in fractional radius. An exception is rotor 8 which has very poor performance at the inner radii at this operating condition, although it is better than the others in the outer region. This rotor had a shroud at the radius of lowest efficiency.

Tentatively we conclude from the general trend that the drop in efficiency near the tips is dependent on geometrical factor, and not only on the high Mach numbers associated with the tips. This is not a new conclusion. It has long been practice[4-6] to use different D factor loss correlations for the near-hub and near-tip radii than for midspan, the effective loss near the tip being several times that at midspan.

To complete the general picture, the overall efficiency of these same rotors is given on Fig. 6 as a function of their tip tangential Mach numbers, M_{TIP}. Where available, the efficiency of the stage is also plotted as a tailed symbol. The efficiency with oblique shocks is included for reference, and as in Fig. 4 it suggests that a substantial efficiency increase should be possible. From Fig. 5 it appears that the improvements must come mainly in the supersonic flow region,

*The techniques of efficiency determination and their limitations are discussed in the next section under Sources of Data.

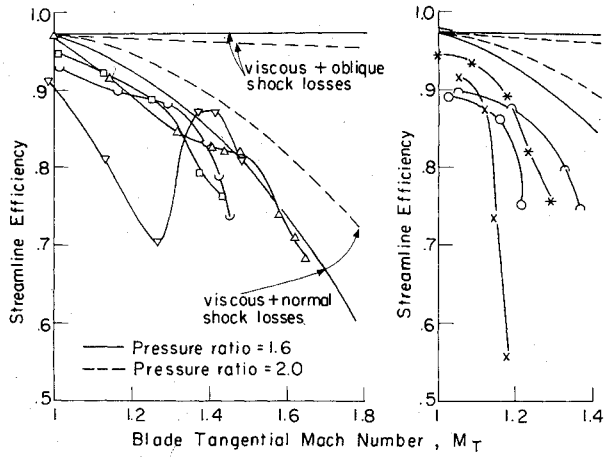

Rotor Number	Tip Mach Number	Hub radius / Tip radius (inlet)	Design Pressure Ratio	Ref.	Symbol
1	1.65	.5	2.34	36	△
2	1.21	.5	1.6	47	○
3	1.41	.312	1.966	48	□
4	1.41	.50	1.686	49	∩
5	1.50	.50	2.00	5	∪
6	1.2	.50	1.60	19	×
7	1.32	.375	1.629	50	*
8	1.52	.46	1.51	11	▽

Fig. 4 Streamline efficiencies for supersonic portions of several transonic rotors (theoretical estimates of losses expected from cascade data, plus shock losses for oblique and normal shocks are given for comparison).

from about 80% radius to the tip. Thus, our task is to understand the mechanisms which control the losses in this region.

Physical Description of the Flow

The rotation, complex geometry, and hostile environment of turbomachines and especially of engines have made the acquisition of detailed information about the flow both difficult and expensive, so that the data bank is not extensive. Some of the information is held in proprietary form by the major aircraft engine manufacturers and cannot be addressed here, where we are limited to information which has been put in the public domain. Some of the best rotors probably fall into this proprietary class. While admitting that these most highly developed rotors may be somewhat better than most of those to be examined here, we are inclined to the view that the major features of the flow in the best rotors will not differ greatly from those to be discussed here and that they, too, will bear improvement.

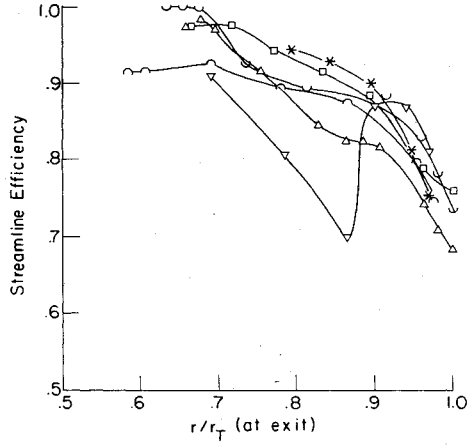

Fig. 5 Streamline efficiencies for rotors of Fig. 4 displayed as functions of radius of streamline at rotor exit divided by tip radius at exit.

Sources of Data

Most of the available data on turbomachinery flowfields are from steady-state measurements made between blade rows with conventional total pressure probes, wedge probes which give flow angles on the mean axisymmetric stream surfaces, stagnation temperature probes, and casing static pressures. These data give little information about blade-to-blade variations in the flow, and none about radial flows which have nearly zero mean values. Peripheral surveys behind stators do give some information about the rotor wake structure,[7] but only by way of a modeling which is not quantitative at present. Otherwise, these data yield peripherally averaged flow angles, stagnation pressures, and stagnation temperatures as functions of radius. From the latter two, the peripherally averaged efficiency is derived, and these are the data shown in Fig. 4.

There is some uncertainty as to the interpretation of steady-state data due to the averaging characteristic of the probes. Weyer[8] has shown by use of an oil-filled stagnation probe that conventional pitot probes have significant errors, depending on the degree of unsteadiness and the Mach number. He found errors of as much as 8% in mean stagnation pressure as seen by a conventional pitot probe near the tip of rotor 2 of Fig. 4 at design speed. At present there is no pressure-measuring instrument which is capable both of time resolving the unsteady flowfield and also giving highly accurate mean values, so the reasons for this discrepancy are not easily resolved.

In some cases the rotor efficiencies reported in Fig. 4 were derived from measurements performed downstream of the stators. This is done sometimes to avoid probe blockage effects on the rotor and sometimes because there is insufficient axial spacing between the rotor and stator to allow introduction of a survey probe. One procedure, following the logic of Ref. 7, is to take the stagnation pressure between stator wakes as the rotor outlet stagnation pressure, and the mass flow average over the stator gap of stagnation temperature as the rotor outlet stagnation temperature. These values are carried back to the rotor outlet along stream surfaces defined by some axisymmetric computation. Clearly any radial transport across the axisymmetric stream surfaces will lead to the inference of incorrect profiles of stagnation pressure and temperature at the rotor outlet.

Data which exhibit the blade-to-blade flows are available for very few rotors. They can be obtained by means of either steady-state instruments operating in rotor coordinates,[9] or by time-resolved measurements in stationary coordinates, the latter having provided most of the information thus far. The point-measuring instruments available include hot-wire anemometers,[7] casing static pressure transducers,[10] high-frequency response multisensor probes,[11,12] and laser anemometers.[14-16] Instantaneous maps of the flowfield can be obtained with holography[17] and with laser-induced fluorescence.[18] Each of these instruments has both advantages and disadvantages. They all share the characteristic that they produce a huge volume of information, which at present is not readily digested and used in the design process.

The other sources of new information are direct numerical computations of the flow, two-dimensional, quasi and fully three-dimensional, and linear three-dimensional theory. Reference to some results of this computational work will be

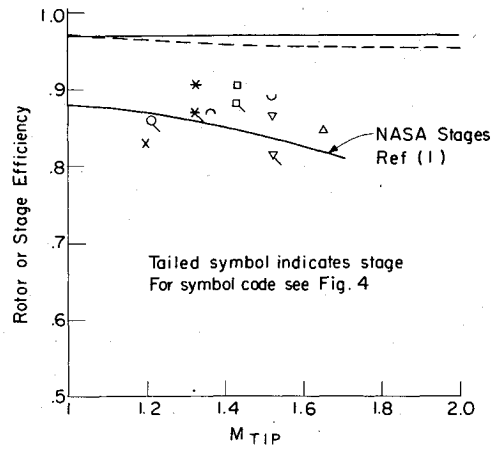

Fig. 6 Rotor and stage efficiencies for rotors of Fig. 4, compared to NASA experience and to theoretical estimate accounting for cascade losses and oblique shock losses.

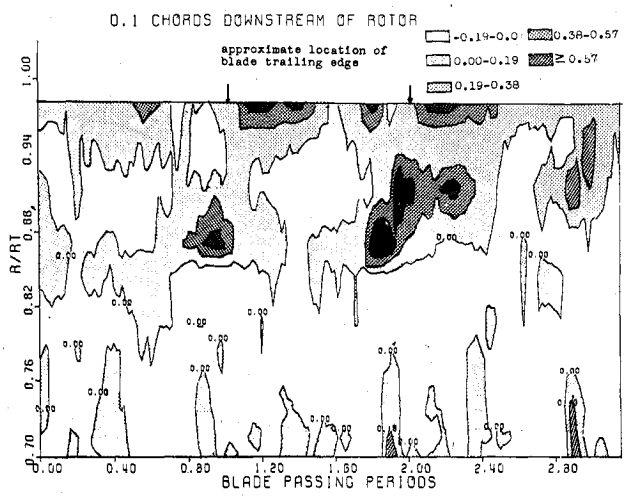

Fig. 7 Radial Mach number at the outlet of rotor 6 of Fig, 4 as a function of radius and peripheral distance, showing islands of large disturbance at blade passing period (from Ref. 19).

made as the physical features of the flow are described. A more complete discussion of the status of the numerical and theoretical work follows in the discussion of modeling capabilities.

Strong Radial Flows in Rotor Wakes

Time-resolved measurements of both radial and tangential flow angle, as well as of static pressure and stagnation pressure,[13,18] in the MIT Blowdown Compressor have shown that the rotor blade wakes just downstream of the blade trailing edges have radial velocities of the same order as the axial or tangential velocities. A map of the radial Mach number as a function of radius and the peripheral coordinate θ shows that the radial velocities are largest in the outer portion of the annulus (Fig. 7). These radial components, although they average nearly to zero in the peripheral mean, can lead to very strong radial coupling in the flow,[20] as will be discussed below. They arise from the radial disequilibrium caused by the difference between tangential velocities in the wake and in the inviscid flow. Very recently, measurements have been made with steady-state instrumentation rotating with a low-speed rotor which also show strong radial components,[9] as had hot-wire measurements in this same compressor.[21]

Being normal to the mean flow direction, these radial flows and the peripheral perturbation velocities which they imply through continuity represent flow kinetic energy which is not recoverable by the mean flow, hence their kinetic energy must

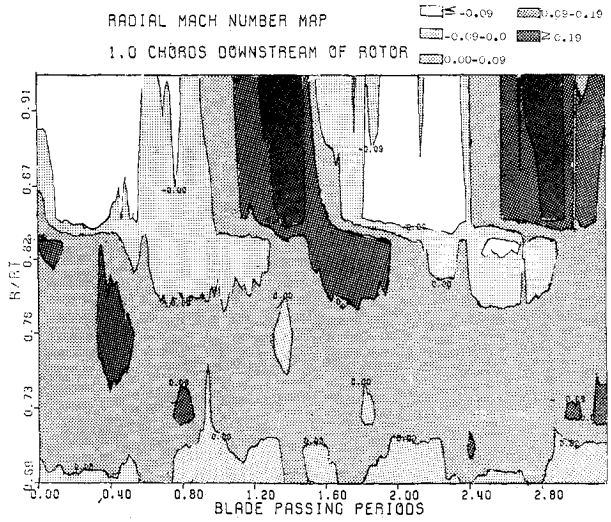

Fig. 8 Radial Mach number one chord downstream of rotor 6 of Fig. 4 showing periodicity at about 1.4 times blade passing period, (from Ref. 19).

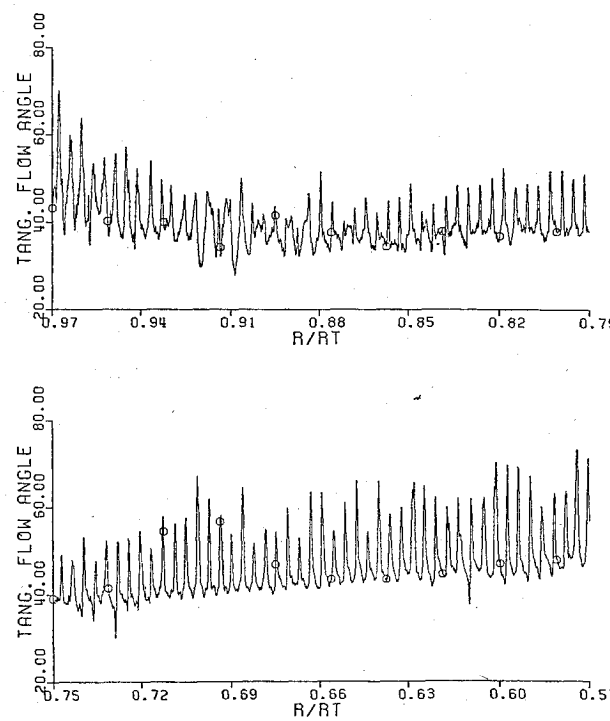

Fig. 9 Tangential flow angle at the outlet of rotor 7 Fig. 4 as function of time, as measured by traversing probe (from Ref. 10).

be considered a contribution to the rotor inefficiency,[20] a point we will return to in the discussion of modeling.

Unsteadiness in Rotor Coordinates

Most theoretical descriptions of rotor flow assume that the flow is steady in rotor coordinates. The early work of Kemp and Sears[22] indicated that the upstream potential flow effects of downstream stators on rotors were quite small. Asymmetrical stagnation pressure distributions produce pressure fields in strongly swirling flows,[23] particularly for low-order disturbances.[24] But there is also considerable evidence that the flow is unsteady in highly loaded rotors even without forcing by such geometric asymmetries.[7,13]

It was argued in Ref. 13 that such unsteadiness could result from a forcing of the rotor flow by pressure fluctuations from inertial waves induced by the rotor wakes in the rotor outflow. Due to its strong swirl the downstream flow is capable

of supporting such waves, which have a peripheral structure dependent on the variation in radius of the mean swirl velocity. In general, the periodicity of this structure will not match that of the rotor outflow, which is controlled by the number of blades, and the result is a forced unsteadiness somewhat akin to a propagating stall, but of smaller amplitude. In Ref. 13 it was reported that the flow evolved from a 23 per revolution periodicity just behind the rotor to 16 per revolution one chord downstream. Figure 8 shows the radial velocity structure at this station. The period of the disturbance is about 1.4 blade passing periods (23/1.4 = 16). At any given time some blade passages are subjected to diffusion requirements more severe than the mean, and may therefore produce higher losses than would be expected for steady flow.

It seems to be quite generally true that the unsteadiness in rotor coordinates is most prominent in the outer portion of the annulus, where the losses are highest. Weyer and Hungenberg[8] reported root-mean-square fluctuations (from steady flow in rotor coordinates) as high as 28% in rotor 2 just outside the sonic radius, and values as high as 44% in a region of poor flow near the hub.

It also seems to be that the level of unsteadiness is lower in rotors with high efficiencies. A complete set of time-resolved measurements of the flowfield of rotor 7 (Fig. 4) has recently been obtained in the MIT Blowdown Compressor Facility.[10] The tangential flow angle β at outlet of this rotor is shown as a function of time in Fig. 9. The abscissa is labeled as radius divided by tip radius because the data were obtained from a probe traversing from tip to hub at a nearly constant rate. Each sharp upward spike represents the wake of a blade passing over the probe. There is considerable variation from blade to blade near the tip, but much less so near the hub.

Shock Structure

Information about the actual shock structure in rotors comes from four sources. Pressure patterns constructed from casing pressure measurements give the pressure distributions in the rotor passages at the tip. These are influenced by tip clearance vortices and by the interaction of the shock pattern with the viscous layer on the casing, but they seem to give reasonable indications of the shock position and strength near the tip. Fig. 10 shows the casing pressure pattern for a rotor with a relative Mach number of 1.65, operating at a pressure ratio of 1.55.[11] It corresponds to rotor 8 of Fig. 4 which showed good efficiency in the outer portion of the radius. But the shock pressure ratios of about 1.4 account for about 2% relative stagnation pressure loss at most, or about 3% inefficiency.

Holographic flow visualization in this same rotor produced records of the shock structure which can be viewed in three dimensions. Any single two-dimensional reproduction of these holograms contains less information, so one seriously interested in fully understanding this rotor is urged to examine the full holograms. They show a strong shock originating on the part-span shroud, which at least partially explains the poor efficiency at $M_T = 1.25$ in Fig. 4. They also show a strong vortex from the tip clearance flow, but this lies too close to the casing to explain the inefficiency at $r/r_T = 0.9$. A photograph of the hologram for this data point is shown in Fig. 11.

Epstein[18] has used a technique of laser-induced fluorescence to obtain quantitative density maps on planes roughly normal to the span in the MIT Transonic Compressor. Two such are shown in Fig. 12, the lower one near the tip and the upper one near the nominal sonic radius. The former shows a lambda shock and a separated region downstream of it, while the latter shows no evidence of separation even though the shock is quite strong, a point to which we shall return.

Laser velocimeters have been employed recently to obtain velocity maps in the rotor passages. Because of data rate limitations, these maps are all obtained by accumulating a set

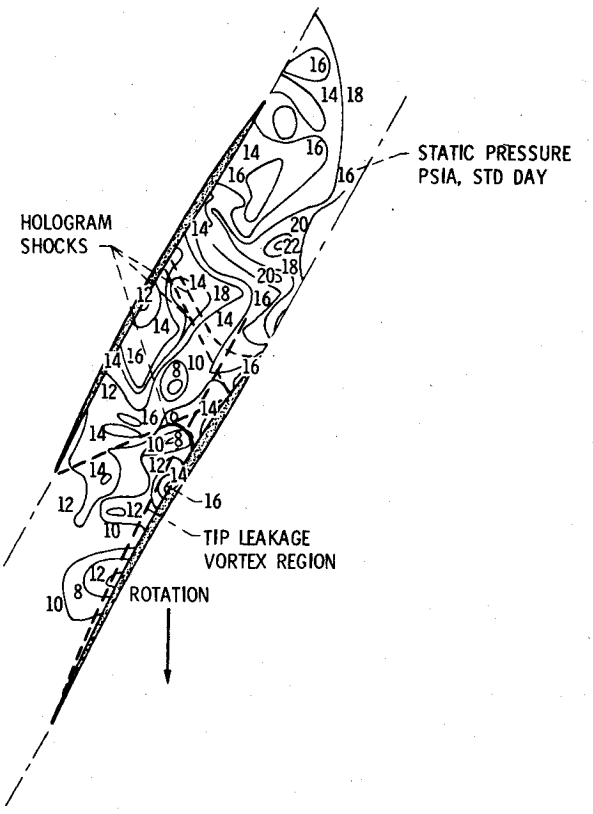

Fig. 10 Casing static pressure distribution deduced from time dependence of set of wall pressure transducers; shock locations as deduced from holograms are shown as dashed lines, as is axis of tip leakage vortex (from Ref. 11).

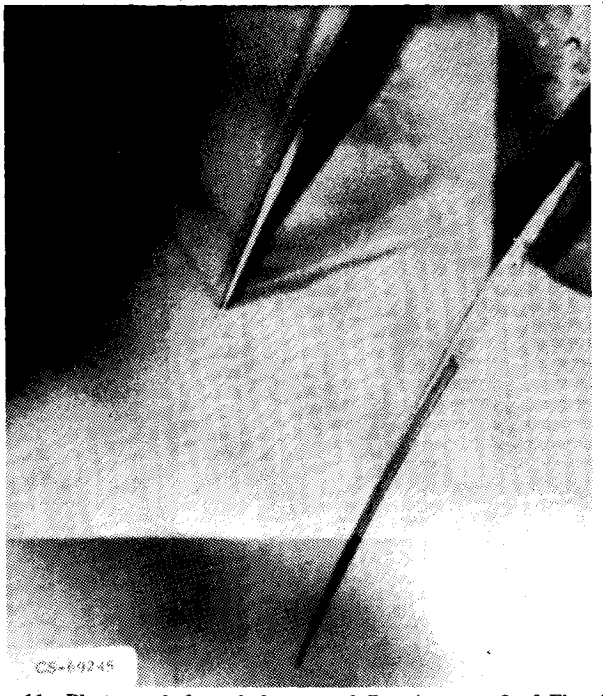

Fig. 11 Photograph from hologram of flow in rotor 8 of Fig. 4, superimposed on blades (from Ref. 17).

of readings taken on successive rotations of the machine, or at least in successive blade passages. Thus they are not instantaneous maps such as are provided by holography or laser fluoresence.

Results obtained by Wisler[14] in a 550 m/s rotor near the tip are reproduced in Fig. 13. They show a double-shock system at a back pressure condition near the normal operating line,

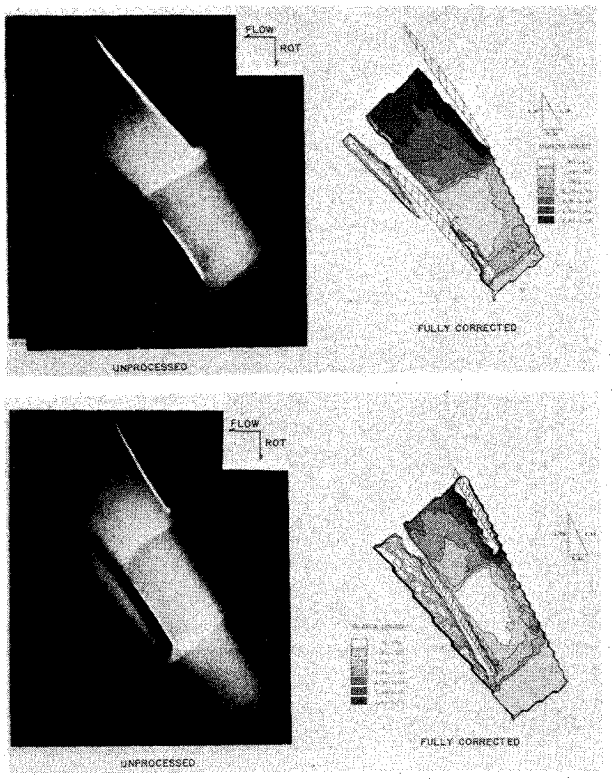

Fig. 12 Density maps of flow in rotor 6 of Fig. 4 for radii near tip (bottom) and at radial location where shock termination strengthens shock and generates strong boundary-layer disturbance (from Ref. 18).

changing to a single stronger shock near stall. Note also the increased Mach number over the suction surface ahead of the shock (1.59 as compared to 1.49) at the high back pressure. As we will see later, the general features of these shocks are well predicted by inviscid computations.

It will be useful to note at this point that although a rotor may be more efficient when operating at a high pressure with a single passage shock, the requirement for adequate surge margin may dictate that it operate normally with a reduced back pressure, and hence with the double-shock pattern. There is a considerable challenge in designing so that the operating point which gives peak efficiency also gives adequate stall margin.

Dunker, Strinning, and Weyer[15] have applied the "L2F" instrument of Schodl[25] to obtain velocity measurements in rotor 2 of Fig. 4. Mach number contours at 89% of blade height are shown in Fig. 14. They show an oblique shock in midpassage, but normal near the two blades, with the midpassage angle near that for maximum flow deflection at the upstream Mach number. From an extensive study of tip pressure patterns Prince[26] has found this condition of maximum deflection to be usual for transonic rotors.

It is worth noting again at this point that the measured shocks in this rotor account for only about 1% stagnation pressure loss which in turn implies about 1.5% in rotor inefficiency. The streamline efficiency of this rotor near the tip is only about 0.75, so the shock loss per se is negligible, as indicated in Fig. 4.

Time-Resolved Rotor Efficiency

From time-resolved measurements of the rotor outflow, a rotor efficiency can be obtained as a function of time on the blade passing time scale, that is, the efficiency is determined for each streamline as it emerges from the rotor. This was first done by Thompkins[19] and reported as an entropy rise map at the rotor exit. Ideally one would measure stagnation temperature and stagnation pressure with sufficient frequency response to resolve the blade wakes, and the instantaneous efficiency would follow directly. In practice, the time-resolved temperature measurement has not been available. The probe used in the MIT Blowdown Compressor provides the stagnation pressure and the three components of Mach number. Thompkins[19] assumed the applicability of the Euler turbine equation to compute the instantaneous stagnation temperature from the tangential velocity. To distinguish this efficiency from the true efficiency determined from a stagnation temperature measurement it will be termed the "Euler efficiency" here.

Recent measurements of the "Euler efficiency" for rotor 7 (Fig. 4) are presented in Fig. 15 on an abscissa labeled radius divided by tip radius, which is the location of a traversing probe, so that the abscissa is really time as in Fig. 9.

Near the hub there are clearly defined regions of low efficiency which can be identified as the blade wakes. Between these are regions where the "Euler efficiency" is near unity, as would be expected of the inviscid flow. On the other hand, near the tip the distinction between wakes and core flow is much less clear, and in fact there are no clearly identifiable regions with efficiency near unity.

A running average in r/r_T of these same data is compared in Fig. 16 with data obtained in steady-state conventional testing of this rotor.[50] and with the design prediction. There is more radial structure in the Euler efficiency as obtained from the Blowdown Compressor, but this may be due to radial transport in the flow through the stator, since as noted above the steady-state measurements were made downstream of the stator. Aside from this the general levels and radial shapes of the efficiency, determined by two completely different techniques, are quite similar.

The significance of the Euler efficiency can be better appreciated by generalizing Thompkins' approach[19] to include a change in rothalpy of the fluid element as it passes through the rotor. The rothalpy is defined as $I=H-\omega rv$ where H is the fluid's total enthalpy, ω is the rotor's angular velocity, r is the radius, and v is the (absolute) tangential velocity of the fluid element. If ΔI_{1-2} represents the change in I, and if v is zero upstream of the rotor, the Euler equation becomes,

$$\frac{T_{t2}}{T_{t1}} - 1 = \frac{\omega r_2 v_2}{c_p T_{t1}} + \frac{\Delta I_{1-2}}{c_p T_1} \tag{5}$$

Now the entropy change across the rotor is

$$\frac{\Delta S_{1-2}}{c_p} = \ell n\left\{1 + \frac{\omega r_2 v_2}{c_p T_{t1}} + \frac{\Delta I_{1-2}}{c_p T_{t1}}\right\} - \ell n\left(\frac{P_{t2}}{P_{t1}}\right)^{\frac{\gamma-1}{\gamma}}$$

Rewriting this and assuming $(\Delta S_{1-2}/c_p) \ll 1$, we find

$$1 + \frac{\Delta S_{1-2}}{c_p} - \frac{\Delta I_{1-2}}{c_p T_{t2}} = \left(1 + \frac{\omega r_2 v_2}{c_p T_{t1}}\right)\left(\frac{P_{t1}}{P_{t2}}\right)^{\frac{\gamma-1}{\gamma}} \tag{6}$$

The Euler efficiency as plotted on Figs. 15 and 16 is based on the value of ΔS_{1-2} computed from this equation, with $\Delta I_{1-2}=0$, whereas in fact what has been determined by measurement of the right side of the equation is $\Delta S_{1-2} - \Delta I_{1-2}/T_{t2}$. Unfortunately, we have at present no means for measuring ΔI_{1-2}, so the actual entropy rise remains uncertain to the extent that ΔI_{1-2} differs from zero.

It will be noted below that the group grad $(S-I/T)$ appears as the representation of the pressure gradient in the Crocco formulation of the total energy equation which is used in streamline curvature calculations.

The source of the high losses near the tip remains a critical question. Equation (6) shows that in the Euler efficiency a change in rothalpy cannot be distinguished from a change in entropy, and only the latter leads to a reduction in efficiency. The rothalpy can change due to viscous interaction or to unsteadiness in rotor coordinates. Thus rothalpy change is

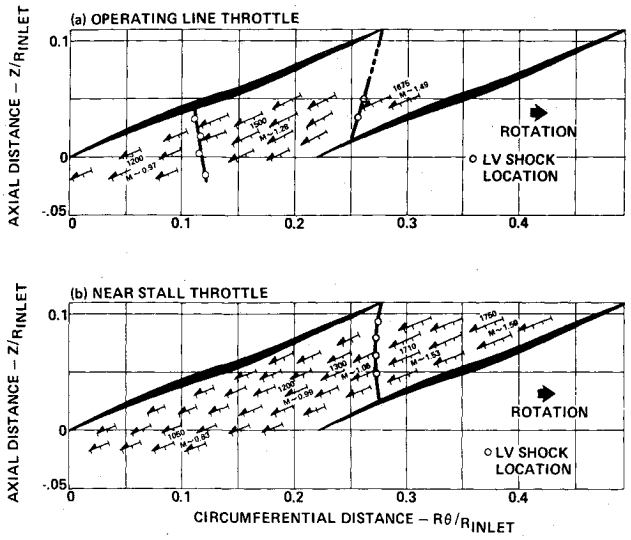

Fig. 13 Velocity structure near tip in 549 m/sec rotor at two throttle conditions, as measured by laser velocimetry: at top rotor is near normal operating condition, at bottom near stall (from Ref. 14).

one possible explanation for the low tip Euler efficiencies shown in Figs. 15 and 16.

For the origin of such rothalpy changes, and for entropy increases larger than can be explained by a combination of cascade losses and shock-induced entropy rise, it seems likely to the author that we must look to the interaction between the shock systems and the viscous flow and to radial transport in the boundary layers and wakes.

Evidence of one such interaction was given by Epstein, Kerrebrock, and Thompkins,[27] based on analysis of data such as that in Fig. 12. This analysis showed that the shock strength in the MIT Transonic Rotor decreased with decreasing radius near the tip, as expected, but then showed a strong peak near the sonic radius. This result is reproduced as Fig. 17. A qualitative explanation of this was offered, based on a calculation of the radial disequilibrium which occurs behind the passage shock due to the radial gradient of relative Mach number. From a simple model where the axial Mach number is assumed constant and the flow aligned to the flat suction surface, as in Fig. 2, it was found that the substantial derivative of radial velocity behind the shock would be discontinuous at the sonic radius, as shown in Fig. 18, jumping from a value of zero just inside it to a value of

$$\frac{r}{a_2^2}\frac{Dv_{r_2}}{Dt}\bigg|_{M_1'=1+\epsilon} = -\frac{4}{\gamma+1}\left(r\frac{dM_1'}{dr}\right)_{M_1'=1+\epsilon} \tag{7}$$

just outside it. Thus for this simple model there is a discontinuity unless the condition $dM_1'/dr = 0$ is satisfied at the sonic radius. The argument then is that the jump in shock pressure ratio results from the accommodation of the flow to remove this discontinuity. Haymann-Haber and Thompkins[28] have since carried the analysis further via three-dimensional computations, as will be discussed in the next section. They have shown that the relative Mach number adjusts so as to produce a local maximum in M_1'. These results are shown in Fig. 19 for locations at the suction and pressure surfaces and in midpassage.

It is argued in Ref. 27 that the sharp pressure gradient produced by this shock termination phenomenon would lead to strong radial flows in the boundary layer, which is unable to withstand the pressure gradients produced in the transonic inviscid flow. The consequent high losses were identified in Ref. 13 in the form of a streamwise vortex.

While the simple model of Ref. 27 assumes the passage shocks are normal, and it can be argued that the shock termination phenomenon might be eliminated by an appropriate obliquity of the shocks as a function of radius, it should be noted that for practical leading-edge radii (as dictated by damage tolerance), there is always a detached shock over the tip of the blade, and the simple model described here applies directly to the flow through these segments of the shock. Detailed laser anemometer studies by Strazisar[16] of the flow in a rotor with tip relative Mach number of 1.4 indicate that the shock has a much larger standoff near the hub than near the tip, as shown in Fig. 20. Perhaps this is due to a radial flow behind the shock resulting from the disequilibrium described above.

Since one key to the excessive losses in the transonic rotor seems to be in the interaction between the shock structure and the viscous flow, more detailed experiments than have been done to date will be required to expose the basic mechanisms to detailed study. The techniques described will require further development, so they are applicable closer to the blades' surfaces, or new techniques must be devised which can define the viscous flow.

Whatever experimental techniques are developed, the flow is so complicated that powerful theoretical and numerical

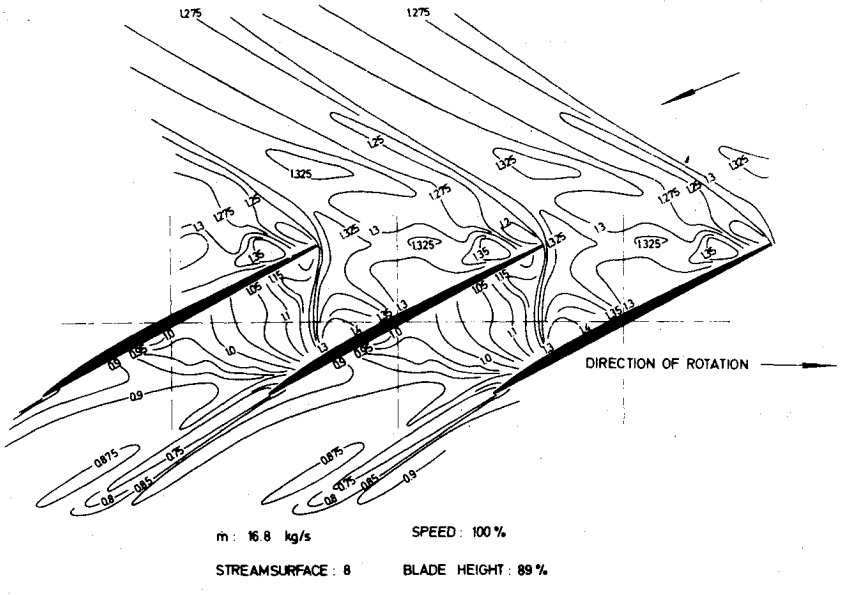

Fig. 14 Mach number contours in rotor 2 of Fig. 4 at design speed and 89% blade height, as found by laser velocimetry (from Ref. 15).

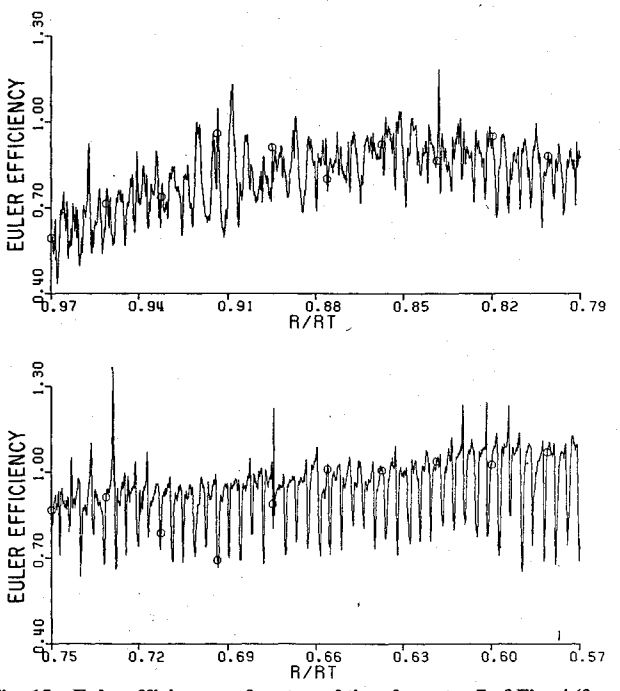

Fig. 15 Euler efficiency as functon of time for rotor 7 of Fig. 4 (from Ref. 10).

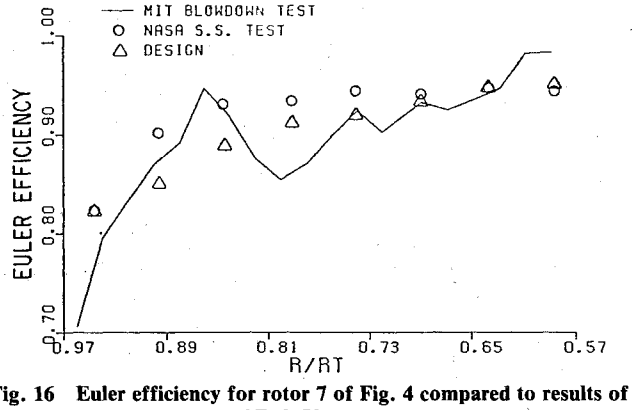

Fig. 16 Euler efficiency for rotor 7 of Fig. 4 compared to results of steady-state measuremens of Ref. 50.

modeling techniques will be required to interpret the data. We next review the state of that art.

Modeling Capabilities

To what extent are we able to model the phenomena described above? The answer to this question must be in two parts, the first applying to the state-of-the-art as practiced by compressor designers and the second to capabilities under development in research efforts.

Design Practice

It is necessary at the outset to restate the caveat that the brief outline of the state of the design practice to be given here is based on the perceptions of one who has not practiced the art, but has attempted to understand it as a basis for working at improvements. The perceptions come from the study of representations of the art in the public domain and may underestimate the sophistication of some industrial design systems.

These design systems are based on an interactive use of approximate models for two features of the flow: namely, first the throughflow, which is approximated as an axisymmetric flow controlled by the hub and tip contours and by peripherally averaged force and loss distributions representing the blading, and second the blade-to-blade flow,

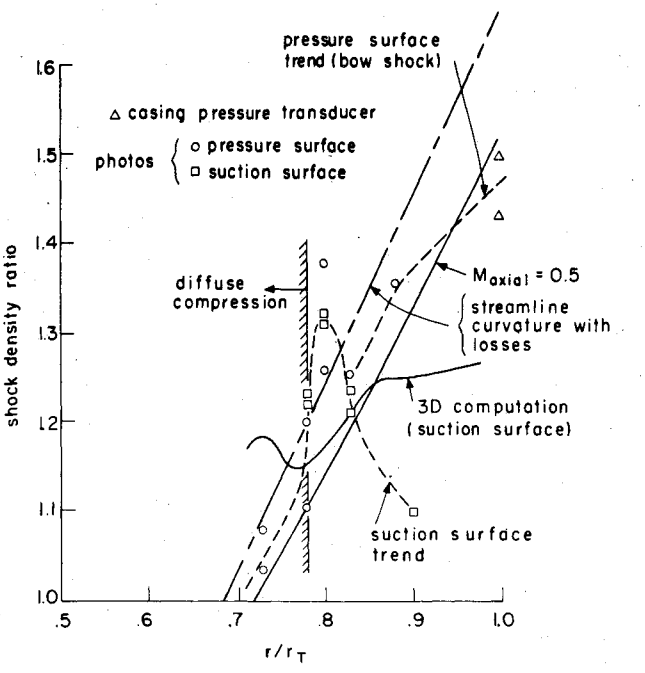

Fig. 17 Density ratios across shock in transonic compressor rotor, showing sudden rise near sonic radius due to shock termination (from Ref. 27).

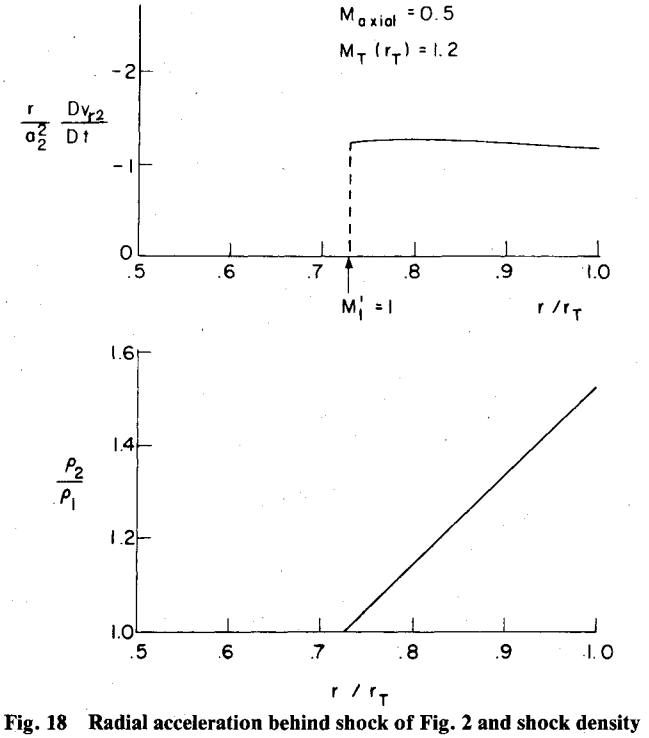

Fig. 18 Radial acceleration behind shock of Fig. 2 and shock density ratio as functions of radius (from Ref. 27).

which is treated as nearly two-dimensional in planes tangent to the axisymmetric stream surfaces. The design proceeds by iteration between these two, the blade-to-blade model providing the flow deflection and loss data to the throughflow, and the latter in turn providing flow velocities and stream tube convergence to the blade-to-blade model. This approach is attributable to Wu,[29] but was not used for design until expanding computational capabilities made the extensive iterations possible.

An overall review of throughflow theory is given by Marsh in Ref. 30. There are two methods in use for solving the axisymmetric flow, the streamline curvature approach of Smith,[31] Novak,[32] and Silvester and Hetherington,[33] and the

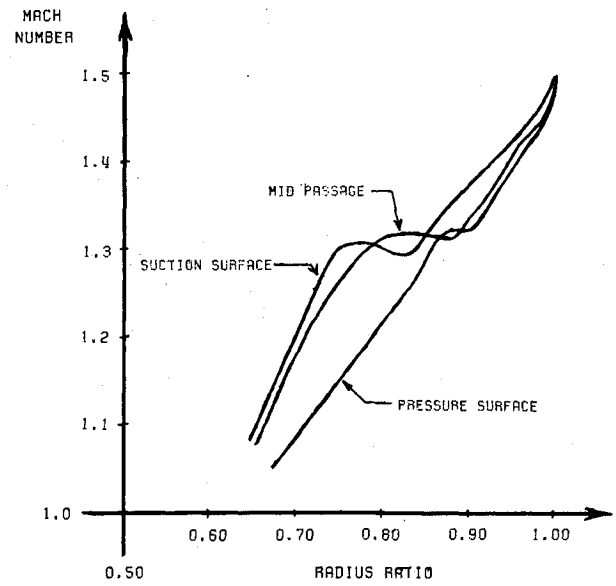

Fig. 19 Mach number ahead of passage shock in MIT Transonic Rotor as found from three-dimensional computation, showing maxima such that condition $dM_1'/dr = 0$ is satisfied (from Ref. 44).

matrix throughflow approach of Marsh.[34] In the first of these the radial momentum equation is solved iteratively with the continuity equation after some of its terms are evaluated by use of the energy equation and the pressure is replaced by the enthalpy and entropy. In the matrix throughflow method continuity is satisfied by introduction of a stream function which then satisfies a second-order equation in the radial-axial plane. The two equations are in Marsh's notation:

1) Streamline curvature:

$$W_m \frac{\partial \bar{W}_m}{\partial r} = -\frac{W_\theta}{r}\frac{\partial}{\partial r}(rv_\theta) - T\frac{\partial s}{\partial r} + \frac{\partial I}{\partial r} - F_r$$

$$-\left[\frac{1-M_z^2}{1-M_m^2}\right]\frac{W_m^2}{R_m \cos\phi} - \left[\frac{M_r^2}{1-M_m^2}\right]\frac{v_\theta^2}{r} + \left[\frac{M_r M_\theta}{1-M_m^2}\right]F_\theta$$

$$+\left[\frac{W_r}{1-M_m^2}\right]\left[\frac{W_m}{R_m}\frac{\partial s}{\partial m} - \frac{W_z}{r}\frac{\partial}{\partial r}(r\tan\phi) - \frac{W_m}{B}\frac{\partial B}{\partial m}\right] \quad (8)$$

2) Matrix throughflow:

$$\frac{\partial^2\psi}{\partial r^2} + \frac{\partial^2\psi}{\partial z^2} = \frac{\partial\psi}{\partial r}\frac{\partial}{\partial r}[\ell n(Br\rho)] + \frac{\partial\psi}{\partial z}\frac{\partial}{\partial z}[\ell n Br\rho]$$

$$+\frac{Br\rho}{W_z}\left[\frac{\partial I}{\partial r} - T\frac{\partial s}{\partial r} - F_r - \frac{W_\theta}{r}\frac{\partial}{\partial r}(rv_\theta)\right] \quad (9)$$

Here W_m is the velocity in the meridional (r,z) plane, R_m is the streamline radius of curvature, ϕ is the slope of the axisymmetric streamsurface, and B is an allowance for blockage by the blades.

These two approaches are physically equivalent. The tangential velocity is computed from the meridional velocity and some expression for the flow angle, derived either from cascade data (e.g., in the form of a deviation angle) or from a blade-to-blade flow solution, or in the "design problem" from a prescribed radial distribution of work. The entropy, which plays a role in specifying the stagnation pressure distribution in radius, is determined from loss correlations. By choice of the radial profile of loss, the computed flow can be brought into agreement with reality in any particular case. It appears to be in the choice of this distribution, which essentially depends on experience, that industrial design systems differ rather widely.

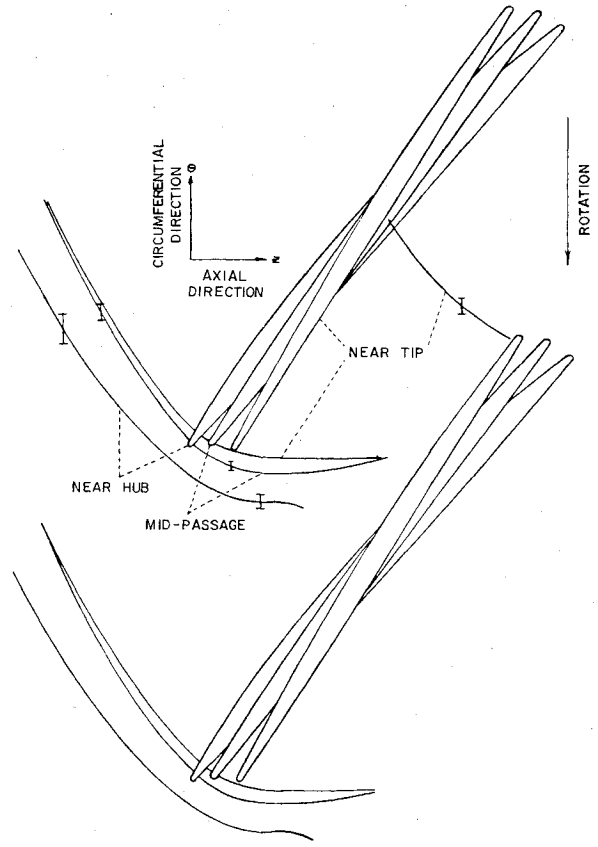

Fig. 20 Shock structure in rotor with tip relative Mach number of 1.40 and pressure ratio of 1.53, as found by laser velocimetry, showing increasing standoff with decreasing radius (from Ref. 16).

Both approaches conventionally assume that the rothalpy I is conserved along the axisymmetric stream surfaces. Physically this is equivalent to saying there is no transfer of energy between adjacent stream tubes except that effected by the forces acting on the blades. As we shall see, this assumption can be in error.

Reference 35 reports an interesting attempt to assess capabilities for throughflow prediction by requesting various turbomachinery experts to predict the flow in machines of specified geometry and rotational speed. The predictions were then compared to the experimental results, the latter having not been available to the modelers. The results of this "quiz" as we would call it in academe were somewhat disappointing. There were serious errors in both pressure ratio and temperature rise.

Reference 5 gives the design expectations for rotor 5 of Fig. 4, clearly one of the most efficient. The streamline curvature method was used in this design, and it achieved its design target for efficiency. This design is a product of one of the more highly tuned design systems, which uses a large backlog of empirical data in estimating the expected loss distribution.

The degree of uncertainty in the loss distribution for high Mach number rotors is well illustrated by the design and test of rotor 1 of Fig. 4. A redesign of this rotor is described in Ref. 36. The original rotor was designed with precompression blading, and gave the efficiency shown in Fig. 4. The redesign[36] is by a quasi three-dimensional procedure in which the radial thickness of axisymmetric stream tubes is accounted for in computing the blade-to-blade flow. Multiple-circular arc blading is proposed for the redesign. Figure 21 from Ref. 36 shows the radial loss distribution for this rotor in terms of total pressure recovery relative to the rotor. It also shows the losses attributed to boundary layers and those due to the shocks. These do not account for the total losses, the remainder being lumped into "residual losses" which are carried over from the old design to the new one and amount to 10% in efficiency from the 75% span outward. It is the origin

of these "residual losses" which must be understood if the efficiency of high Mach number compressors is to be improved. Interestingly enough, the authors of Ref. 36 state that the philosophy for optimization of the rotor design is to minimize the shock losses, but from Fig. 21 we see that the shock losses per se as predicted by their design system do not make up a major part of the losses in the outer portion of the annulus.

Developing Capabilities

Current attempts to improve the predictive capability may be divided roughly into three classes: attempts to improve the axisymmetric design systems, analytical theories based on linearization about the mean axisymmetric flow, and direct numerical attacks on the full three-dimensional problem.

Axisymmetric

Sehra and Kerrebrock[20] have developed a method for incorporating the effect of blade-to-blade flow variations from the mean axisymmetric flow in the streamline curvature method as developed by Hearsey.[37] The method recognizes the "apparent stresses" which appear in the equations of motion as a result of peripheral averaging of the nonlinear terms. These effects were noted by Smith[31] and Hirsch[38] but were found to make small contributions to the radial momentum equation. These same stress terms do, however, lead to variation along stream surfaces of the rothalpy based on mean flow quantities, as demonstrated in Ref. 20 by averaging of the energy equation. This variation has a powerful effect on the mean flow.

The equation for the rothalpy takes the form,

$$\frac{\bar{D}\bar{I}}{Dt} = -\left[\bar{W}_r\left(\Sigma_r + \frac{\overline{w_\theta'^2}}{r}\right) + \bar{W}_\theta\Sigma_\theta + \bar{W}_z\Sigma_z - \Phi_{app} + \frac{\bar{D}}{Dt}\left(\frac{\overline{w'^2}}{2}\right)\right] + \text{other terms} \tag{10}$$

where Σ_r, Σ_θ, and Σ_z are the radial, tangential, and axial apparent stresses, e.g.,

$$\Sigma_r = \frac{\partial}{\partial r}(rw_r'^2) + \frac{\partial}{\partial z}(\overline{w_r'w_z'}) - \frac{\overline{w_\theta'^2}}{r}$$

and Φ_{app} is the effective dissipation due to these stresses.

Sehra and Kerrebrock[20] also define an "apparent entropy" which accounts for the fact that flow energy, which is invested in perturbations of a length scale which cannot be recovered by the blade rows, is effectively lost to the mean flow and thus should be considered a contribution to the thermal energy of the gas. The expression for the apparent entropy takes the form,

$$T\frac{DS_{app}}{Dt} = \frac{D(\overline{w'^2})}{Dt} + \Phi_{app} \tag{11}$$

These improvements were tested by using the measured blade-to-blade flow found in the MIT Blowdown Compressor to compute the additional terms. The degree of success in the prediction can be seen from Fig. 22. Here the tangential velocity at outlet from rotor 6 of Fig. 4 is compared to predictions of three types. In the figure at the left, the solid line gives the results of the streamline curvature calculation, with cascade losses based on the D factor correlation.[3] The dashed line gives the mean flow found from the full three-dimensional inviscid computation of Thompkins.[19] It is seen that they are very similar, and that they both miss the major features of the radial variation in tangential velocity. At the right is the prediction including the effects of apparent stresses, rothalpy variation, and apparent entropy variation. It very well predicts the observed variation even to the local

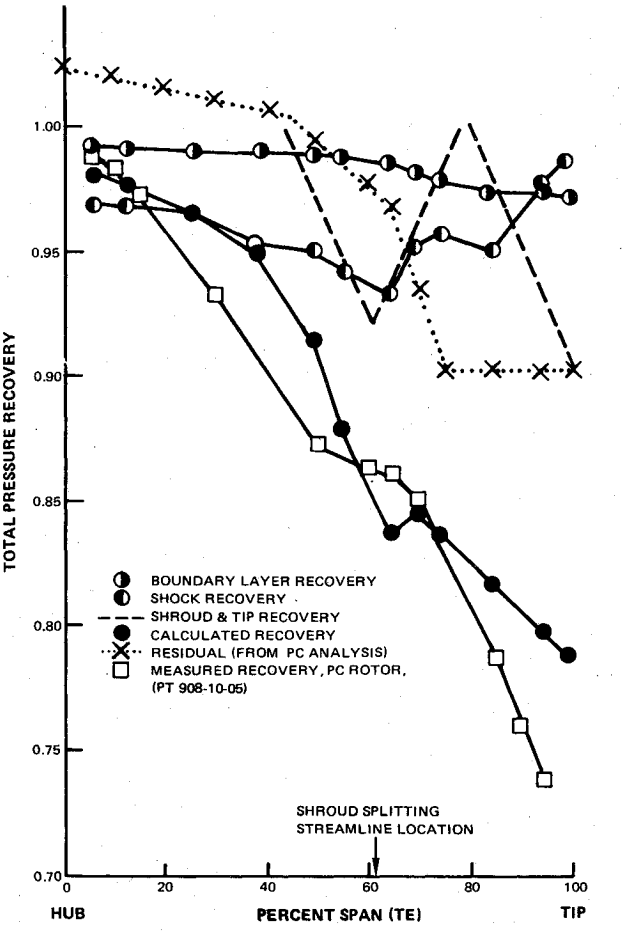

Fig. 21 Radial profiles of measured totoal pressure recovery in rotor coordinates for rotor 1 of Fig. 4 and predictions for multiple circular arc redesign of this rotor; note empirical "residual loss" which is carried from one design to next (from Ref. 36).

maximum at midspan, which is thought to stem from the shock termination phenomenon discussed above. Note that the magnitude of v_θ is set by the mass flow, which was not matched correctly in these comparisons. But shifting it would not change the shape of the computed curves very much. We conclude from this comparison that the effects of rothalpy and apparent entropy variation are very important. But more than that, these quantities are largely controlled by the viscous flowfield, since their inviscid effect should be included in the three-dimensional inviscid solution at the left in Fig. 22.

In addition to this direct computation from the velocity fluctuations, Sehra computed the axisymmetric flow using essentially Eq. (8) with $\overline{\partial I}/\partial r = 0$ and with $\overline{\partial s}/\theta r$ given by the entropy rise reported by Thompkins. This yielded excellent agreement between the computed and measured radial distributions of tangential velocity, even better than that shown in Fig. 22. The reason for this can be seen from Eq. (6). The entropy rise reported by Thompkins[19] is given by the right side of Eq. (6), since the assumed $\Delta I_{1-2} = 0$. But in fact the right side of Eq. (6) gives the combination $\Delta S_{1-2} - \Delta I_{1-2}/T_{t-2}$, which is exactly the desired input to Eq. (8). This has some practical importance for the prediction of axisymmetric flows using empirical data. Since the profiles of v_2 and P_{t2} are readily measurable it is easier to determine the group $\Delta S_{1-2} - \Delta I_{1-2}/T_{t2}$ than to determine ΔS_{1-2} itself, which is usually taken as an approximation to this combination, ΔI_{1-2} being assumed zero.

Linear Theory

By representing the blade-to-blade flows as perturbations about an axisymmetric mean flow with large turning and arbitrary radial variations, the linear theories offer the

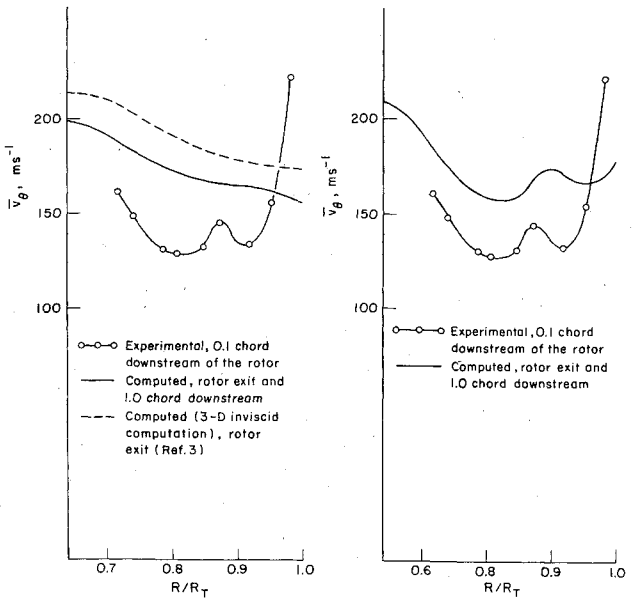

Fig. 22 Comparison of measured outlet tangential velocity of rotor 6 with predictions by three methods: conventional streamline curvature with cascade losses and three-dimensional inviscid computation at left and, accounting for apparent stresses, rothalpy an apparent entropy variation at right (from Ref. 20).

possibility of studying, for example, the change in blade incidence due to the vorticity shed in the blade wakes.[39] This vorticity can arise due to radial variations in the blade circulation[40] or due to viscous effects. In the latter case the theory is not closed, since it cannot describe the process of generation of the vorticity, but rather only its effects on the flow after it is produced.

The linearized theory is capable of describing most efficiently the general small-disturbance field in the swirling flow of a turbomachine. A first attempt at such a description in modal form was made by Kerrebrock,[23] who showed that the behavior of shear disturbances depended markedly on the character of the mean swirl. Wheel-type flows support persistent oscillations with pressure disturbances coupled to the vorticity, while free vortex flows and those with mean circulation decreasing outward tend to exhibit decaying disturbance fields. Adebayo[41] has developed a treatment of Beltrami flow with arbitrary mean swirl, which shows that these two types of behavior can coexist in different radial locations of the same turbomachine annulus. This agrees with the experimental finding of Thompkins and Kerrebrock.[13]

Numerical approaches to the three-dimensional flow all suffer from limitations on the number of grid points available, and these must be allocated between the upstream flowfield, the flow in the blade passages, and the downstream flow. Accurate representation of the conditions far upstream and downstream can require a significant fraction of the total, particularly if proper treatment of the convected downstream disturbances is required. Since the perturbations are small in the upstream and downstream flows they can be accurately represented by the linear theory, which can be matched to numerical solutions at planes just upstream and downstream of the blade row. Thus a combination of linear theory and direct numerical computation may prove to be the most efficient approach to turbomachine flowfields. This approach was used for the upstream flow by Haymann-Haber and Thompkins.[28] It gives promise of direct computation of the upstream noise field of transonic rotors for example.

Computational Fluid Dynamics

Direct numerical solutions to the three-dimensional flow offer the only apparent means to understand fully the complicated flow in compressor blade rows. The effects of

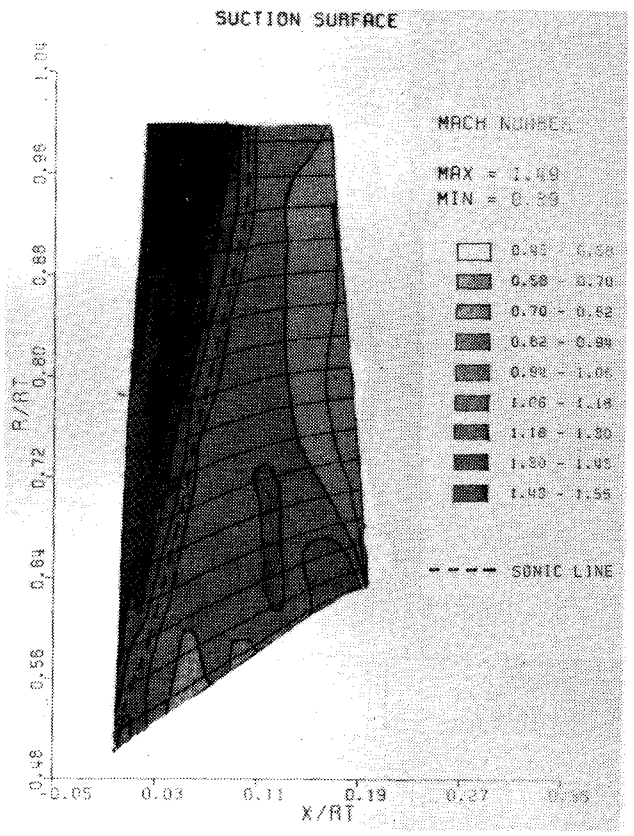

Fig. 23 Constant Mach number contours on suction surface of rotor 6, as predicted by three-dimensional computation (from Refs. 28 and 41).

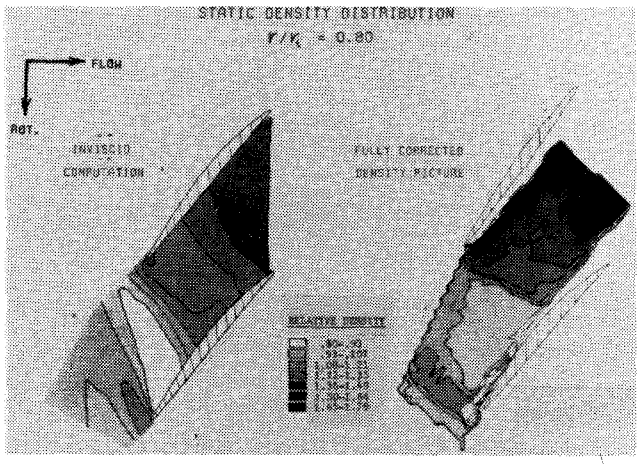

Fig. 24 Comparison of density distribution predicted by three-dimensional computation with measurements by gas fluorescence (from Refs. 28 and 44).

radial variation in relative Mach number and blade relative stagnation pressure, strong swirl, and the sensitivity of transonic flow to small geometrical variations combine to make an accurate prediction of the blade surface pressure distributions unattainable without a full three-dimensional treatment.

The first attempt at a direct numerical solution of a flow containing the essential features of the transonic compressor was made by Oliver and Sparis,[42] who computed by a time-marching procedure the flow in a rectilinear cascade with a spanwise variation of relative Mach number from 0.8 at one wall to 1.2 at the other. This calculation showed that the shock pressure rise at the high Mach number end produced a strong spanwise flow toward the low Mach number end, with

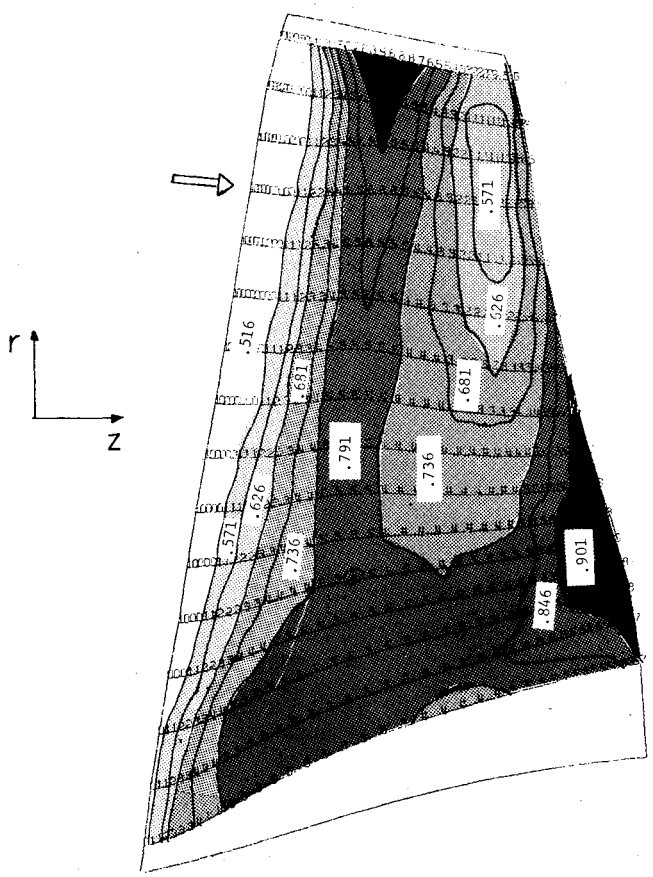

Fig. 25 Constant pressure contours on the suction surface of rotor 7 of Fig. 4, showing strong passage shock followed by re-expansion and second shock near tip; inset numbers are pressure in atmospheres (from Ref. 45).

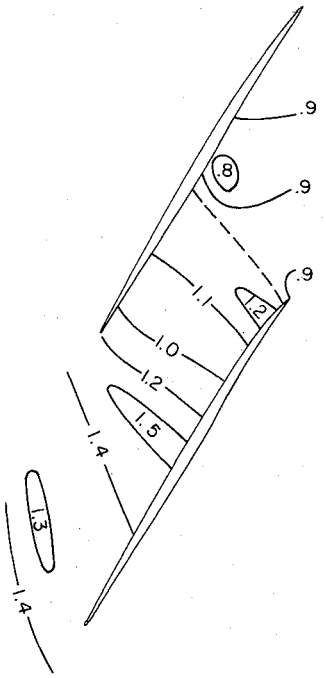

Fig. 26 Mach number contours near the tip for rotor 7 of Fig. 4, showing double-shock configuration (from Ref. 45).

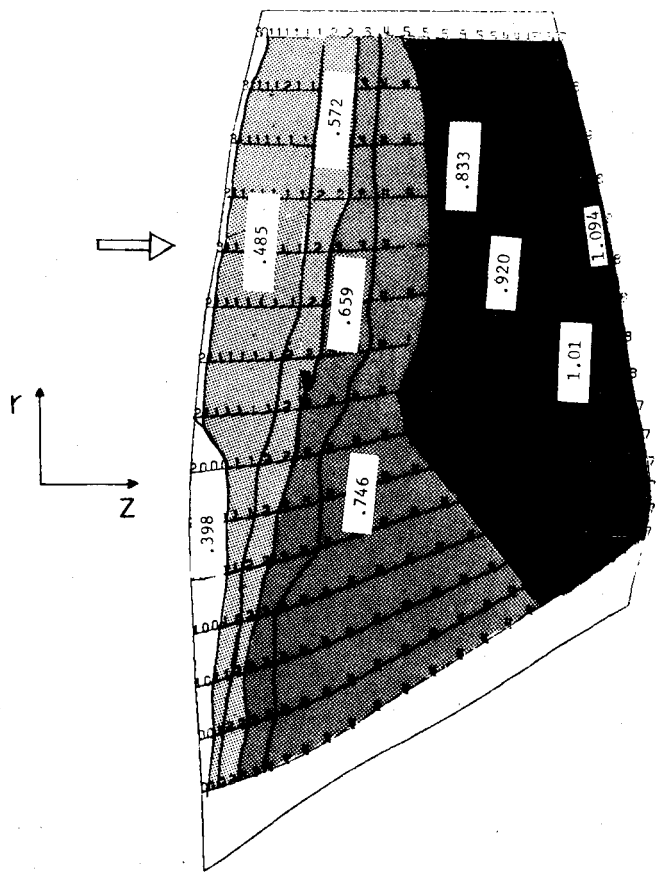

Fig. 27 Constant pressure contours on suction surface of rotor 3 of Fig. 4, with smooth gradual compression followed by shock at passage exit; inset numbers are pressure in atmospheres (from Ref. 45).

a resulting increase in Mach number in the subsonic zone and in the supersonic zone as well. This is the same effect alluded to above in the discussion of shock structure. It is undoubtedly present to some extent in all transonic compressors, and is not dealt with by the design systems in current use.

The same time-marching procedure was also applied by Sparis[43] to compute the flow in the MIT Transonic Compressor Rotor, but his solution was for a mass flow condition which led to a very low pressure ratio and so was not suitable for comparison to experiment. Thompkins improved some aspects of the computational procedure, notably the treatment of boundary conditions, and carried a solution to completion for a mass flow close to the best operating point for the rotor.[19] He compared his results to time-resolved measurements at the rotor outlet and also to the gas fluorescence density maps of Epstein.[18]

The computation of the flow in the MIT rotor was carried to a higher level of precision by Haymann-Haber,[44] with finer grid resolution and inclusion of the energy equation in place of the assumption of isentropic flow. This computation yielded results such as those shown in Fig. 23 where Mach number contours on the suction surface show, for example, that sonic flow extends nearly to the hub. The nominal upstream sonic radius is $r/r_T = 0.70$. The comparison in Fig. 24 of the computed density profiles at $r/r_T = 0.80$ with those measured by Epstein[18] shows good agreement in the strength and location of the passage shock at the pressure surface, but a significant difference near the suction surface, where the shock/boundary-layer interaction discussed above occurs. This computation also led to Fig. 19. Thus it does appear that this computational approach gives an accurate representation of the inviscid flow.

Solutions have been produced by Thompkins[45] with this code implemented on a PDP-11/70 computer, for three rotors in addition to the MIT Transonic Rotor. The suction surface pressure contours for rotor 7 of Fig. 4 are shown in Fig. 25. They indicate an expansion behind the leading edge followed by a shock compression and then a re-expansion followed by a second shock. This is hardly ideal from the standpoint of

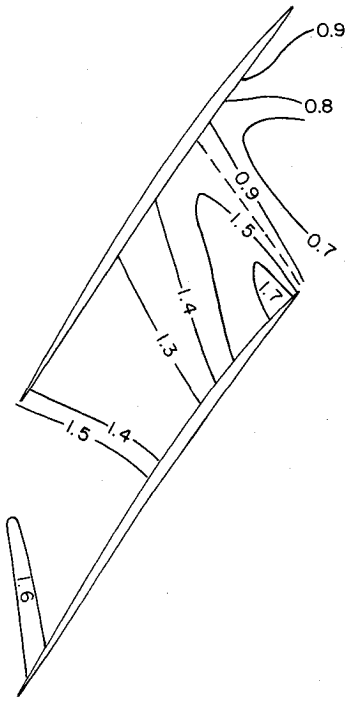

Fig. 28 Mach number contours near tip of rotor 3 of Fig. 4 (from Ref. 45).

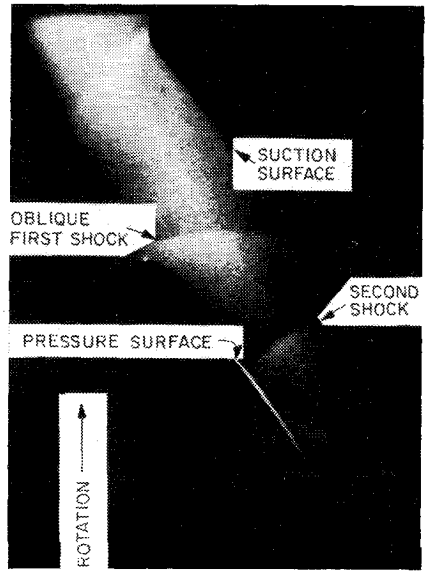

Fig. 29 Density map obtained by gas fluorescence for near-tip region of rotor 3 of Fig. 4; compare to Fig. 28 (from Ref. 47).

optimizing boundary-layer behavior. Looking more closely at Fig. 5 we see that the efficiency of this rotor drops off suddenly from about $r/r_T = 0.9$ to the tip, in the region where Fig. 25 shows an especially severe shock and re-expansion followed by a second shock.

A cross plot of the solution in terms of Mach number for the stream surface having $r/r_T = 0.95$ at the leading edge (Fig. 26) shows a re-expansion from the sonic condition behind the first shock to a Mach number of 1.28, whereupon the flow shocks down to a Mach number of about 0.8, corresponding roughly to a normal shock. But note that this shock would in itself produce only a 2% stagnation pressure loss, while the upstream shock, which has the Mach number change for maximum flow deflection (10 deg) and a pressure ratio of about 1.8, would account for another 2%.

Similar suction surface pressure contours are shown for rotor 3 in Fig. 27. They show a remarkably smooth and gentle suction surface pressure rise, followed by a strong shock at

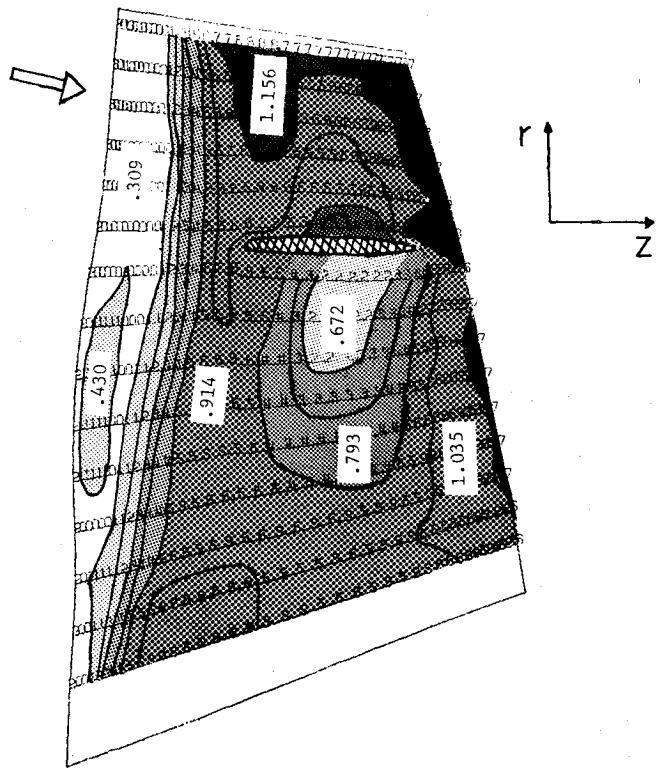

Fig. 30 constant pressure contours on the suction surface of rotor 1 of Table 1, showing strong passage shock over entire span and expansion and recompression under part-span shroud; inset numbers are pressure in atmosphere (from Ref. 45).

the trailing edge which extends halfway to the hub. From Fig. 5, one can see that there is a rather sudden downward break in the efficiency at $r/r_T = 0.7$, which corresponds to this radius.

Figure 28 shows the Mach number contours for this rotor on the stream surface with $r/r_T = 0.95$ at the leading edge. To add credibility to these calculations, Fig. 29 is a fluorescent density map[46] taken by Epstein for this same rotor near the tip. It clearly shows the double shock system.

Finally, Fig. 30 shows isobars for rotor 1, which has a part-span shroud and a very high tip Mach number. It evidently has a strong passage shock following a sudden expansion behind the leading edge, then nearly constant pressure back to the trailing edge. The shroud produces a strong expansion on its underside, perhaps due to a radial inflow on the suction surface stemming from the radial gradient of shock strength described earlier. This most likely could be avoided by use of the three-dimensional computational procedure, if in fact it exits in the actual flow.

Conclusion

A major conclusion from this review is that a large portion of the apparent inefficiency in the supersonic flow zone of transonic compressor rotors is not rationalized by viscous and shock loss mechanisms as they are incorporated in existing compressor design systems. Therefore, these losses are not subject to logical minimization by these design systems.

Since the actual losses exceed the sum of the maximum expected shock losses and the viscous losses which could be expected in the absence of shock interaction, it seems that they must arise in large part from the unfavorable interaction of the viscous flow with the shock system. Detailed measurements and three-dimensional computations for the MIT Transonic Rotor and for a NASA Low Aspect Ratio Rotor support this conclusion. The flow in the region of high loss is characterized by unsteadiness and by large spanwise flows, the effects of which are not included in conventional design systems.

Systematic attempts to improve the efficiency of transonic compressors must be based on studies of the shock/viscous interaction in sufficient detail to delineate the mechanisms of loss generation. While recent results from high-frequency measurements and optical techniques such as laser velocimetry, fluorescent density measurement, and three-dimensional computations are encouraging, much remains to be done before compressor flows can be treated as quantitatively as are external flows.

But the tools are nearly at hand. Methods have been developed for measuring the flowfields between blade rows with enough resolution to define the losses. Optical techniques exist for mapping the velocity and density field in the rotor passages. Their resolution needs to be extended to better examine the details of the viscous flow and its interaction with the shocks. Time-resolved measurements of rotor outlet temperature are needed to resolve uncertainties about the variation of rothalpy. A method is available for accounting for blade-to-blade flow perturbations in computing the axisymmetric mean flow. It is now possible to compute the three-dimensional inviscid flow in a blade row of arbitrary geometry at a cost of only a few hundred dollars, and this cost is dropping rapidly. Soon it will be possible to include viscous effects in such calculations by turbulence modeling. Modern measurement techniques of laser velocimetry, fluorescent density measurement, and high-frequency pressure measurement make possible the detailed investigation of the flowfield which is essential to verification of these better modeling capabilities. These techniques and others must be further developed and extensively applied to study the flowfields of state-of-the-art transonic compressors. Once verified by such experiments, the modern computational techniques should provide a powerful design tool.

It should then be possible to tailor the blade shapes so as to optimize the behavior of the viscous flow, while still meeting requirements for minimum flow area to avoid choking, for structural integrity, and for stability. Such locally optimized shapes should replace the parametrically specified multiple circular arc sections now in use. Boundary-layer control at shock locations on the suction surface may be necessary for optimum performance, as it is in supersonic inlets.

The work which has been reviewed here is certainly only a small start on this formidable task. The possibility exists for improvements in transonic compressors which will yield reductions in fuel consumption comparable to those which the turbofan itself offered relative to the turbojet, but their realization will require a widespread acceptance of these modern techniques by the engine research and development community.

References

[1] For an historical sketch, see Serovy, G. K., "Axial Compressor Aerodynamics," *The Aerothermodynamics of Aircraft Gas Turbine Engines*, edited by G. C. Oatges, AFAPL-TR-78-52, July 1978, Chap. 17.

[2] Chapman, D. R., "Computational Aerodynamic Development and Outlook," AIAA Paper 79-0129, Jan. 15-17, 1979.

[3] Leiblein, S., "Experimental Flow in Two-Dimensional Cascades," *Aerodynamic Design of Axial Flow Compressors*, NASA SP-36, 1965, Chap. VI.

[4] Robbins, W. H., Jackson, R. J., and Lieblein, S., "Blade Element Flow in Annular Cascades," *Aerodynamic Design of Axial Flow Compressors*, NASA SP-36, 1965, Chap. VII.

[5] Sulam, D. H., Keenan, M. J., and Flynn, J. T., "Single-Stage Evaluation of Highly-Loaded High-Mach-Number Compressor Stages II Data and Performance Multiple-Circular-Arc Rotors," NASA CR-72694, July 1970.

[6] Tesch, W. A. and Doyle, V. L., "Evaluation of Range and Distortion Tolerance for High Mach Number Transonic Fan Stages," NASA CR-72786, Jan. 1971.

[7] Kerrebrock, J. L. and Mikolajczak, A. A., "Intra-Stator Transport of Rotor Wakes and Its Effect on Compressor Performance," *Journal of Engineering for Power*, Oct. 1970, p. 359.

[8] Weyer, H. B. and Hungenberg, H. G., "Analysis of Unsteady Flow in a Transonic Compressor by Means of High-Response Pressure Measuring Techniques," *Unsteady Phenomena in Turbomachinery, AGARD Conference Proceedings 177*, Sept. 22-26, 1975.

[9] Sitaram, N., Lakshminarayana, B., and Ravindranath, A., "Conventional Probes for the Relative Flow in a Rotor Blade Passage," *Measurement Methods in Rotating Components of Turbomachinery*, ASME, March 1980.

[10] Ng, Wing-Fai, "Detailed Time Resolved Measurements and Analysis of Unsteady Flow in a Transonic Compressor," M.S. Thesis, Dept. of Mechanical Engineering, Massachusetts Institute of Technology, Cambridge, Mass., Sept. 1980.

[11] Ware, T. C., Kobayashi, R. J., and Jackson, R. J., "High Tip Speed, Low Loading Transonic Fan Stage," Part 3—Final Rept., NASA CR 121263, Feb. 1974.

[12] Kerrebrock, J. L., Epstein, A. H., Haines, D. M., and Thompkins, W. T., "The MIT Blowdown Compressor Facility," *Journal of Engineering for Power*, Vol. 96, No. 4, Oct. 1974, pp. 394-405.

[13] Thompkins, W. R., Jr., and Kerrebrock, J. L., "Exit Flow From a Transonic Compressor Rotor," *Unsteady Phenomena in Turbomachinery*, AGARD Conference Proceedings 177, Sept. 22-26, 1975.

[14] Wisler, D. C., "Shock Wave and Flow Velocity Measurements in a High Speed Fan Rotor Using the Laser Velocimeter," ASME Paper 76-GT-49, 1976.

[15] Dunker, R. J., Strinning, D. E., and Weyer, H. B., "Experimental Study of the Flow Field Within a Transonic Axial Compressor Rotor by Laser Velocimetry and Comparison With Through-Flow Calculations," ASME Paper 77-GT-28, March 1977.

[16] Strazisar, A. J. and Powell, J. A., "Laser Anemometry Measurements in a Transonic Axial-Flow Compressor Rotor," ASME, New Orleans, La., March 5-13, 1980.

[17] Benser, W. A., Bailey, E. E., and Gelder, T. F., "Holographic Studies of Shock Waves Within Transonic Fan Rotors," ASME Paper 74-GT-46, March 31-April 4, 1974.

[18] Epstein, A. H., "Quantitative Density Visualization in a Transonic Compressor Rotor," *Journal of Engineering for Power*, Vol. 99, July 1977, pp. 460-475.

[19] Thompkins, W. T., "An Experimental and Computational Study of the Flow in a Transonic Compressor Rotor," Ph.D. Theseis, Massachusetts Institute of Technology, Cambridge, Mass., June 1976; also MIT GTL Rept. 129, May 1976.

[20] Sehra, A. K. and Kerrebrock, J. L., "The Effect of Blade-to-Blade Flow Variations on the Mean Flow-Field of a Transonic Compressor," AIAA Paper 79-1515, July 23-25, 1979.

[21] Raj, R. and Lakshminarayana, B., "Three-Dimensional Characteristics of Turbulent Wakes Behind Rotors of Axial-Flow Turbomachinery," *Journal of Engineering for Power*, Vol. 98, April 1976, pp. 218-228.

[22] Kemp, N. H. and Sears, W. R., "Aerodynamic Interference Between Moving Blade Rows," *Journal of the Aeronautical Sciences*, Vol. 20, Sept. 1953, pp. 585-598.

[23] Kerrebrock, J. L., "Small Disturbances in Turbomachine Annuli with Swirl," *AIAA Journal*, Vol. 15, June 1977, pp. 794-803.

[24] Greitzer, E. M. and Strand, J. M., "Asymmetric Swirling Flows in Turbomachine Annuli," *Journal of Engineering for Power*, Vol. 100, Oct. 1978, pp. 618-629.

[25] Schodl, R., "Laser Dual-Beam Method for Flow Measurements in Turbomachines," ASME Paper 74-GT-157, March-April 1974.

[26] Prince, D. C., Jr., "Three-Dimensional Shock Structures for Transonic/Supersonic Compressor Rotors," AIAA Paper 79-0043, 1979.

[27] Epstein, A. H., Kerrebrock, J. L., and Thompkins, W. T., Jr., "Shock Structures in Transonic Compressor Rotors," *AIAA Journal*, Vol. 17, April 1979, pp. 375-379.

[28] Haymann-Haber, G. and Thompkins, W. T., Jr., "Comparison of Experimental and Computational Shock Structure in a Transonic Rotor," ASME Paper 80-GT-81, New Orleans, March 1980.

[29] Wu, C. H., "A General Theory of Three-Dimensional Flow in Subsonic and Supersonic Turbomachines in Axial, Radial and Mixed Flow Types," NACA TN 2604, Jan. 1952.

[30] Marsh, H., "Through-Flow Calculations in Axial Turbomachinery: A Technical Point of View," *Through-Flow Calculations in Axial Turbomachinery*, AGARD Conference Proceedings 195, May 20-21, 1976.

[31] Smith, L. H., "The Radial Equilibrium Equation of Turbomachinery," *Transactions of ASME*, Series A, Vol. 88, 1966.

[32] Novak, R. A., "Streamline Curvature Computing Procedures for Fluid Flow Problems," ASME Paper 66-WA/GT-3, 1966.

[33] Silvester, M. E. and Hetherington, R., "Three Dimensional Compressible Flow Through Axial Flow Turbomachines," *Numerical Analysis—An Introduction*, Academic Press, New York, 1966.

[34] Marsh, H., "A Digital Computer Program for the Through-Flow Fluid Mechanics in an Arbitrary Turbomachine Using a Matrix Method," NGTE Rept. R282, 1966; also, Aeronautical Research Council, R&M 3509, 1968.

[35] Weyer, H. B. and Dunker, R., "Comparison Between the Calculated and the Experimental Results of the Compressor Test Cases," *Through-Flow Calculations in Axial Turbomachinery*, AGARD Conference Proceedings 195, May 20-21, 1976.

[36] Norton, J. M., Tari, U., and Weber, R. M., "Rotor Redesign for a Highly Loaded 1800 ft./sec. Tip Speed Fan," NASA CR-159596, April 1979.

[37] Hearsey, R. M., "A Revised Computer Program for Axial Compressor Design," Vols. I and II, Aerospace Research Laboratory, ARL-TR-75-0001, AD A009157, 1976.

[38] Hirsch, C., "Unsteady Contributions to Steady Radial Equilibrium Flow Equations," AGARD Conference Proceedings 177, Sept. 22-26, 1975.

[39] McCune, J. E. and Hawthorne, W. R., "The Effects of Trailing Vorticity on the Flow Through Highly Loaded Cascades," *Journal of Fluid Mechanics*, Vol. 74, Pt. 4, April 1976.

[40] Chen, L. T. and McCune, J. E., "Comparison of Three-Dimensional Quasi-Linear Large Swirl Theory with Measured Outflow from a High Work Compressor Rotor," Massachussetts Institute of Technology, GTL Rept. 128.

[41] Adebayo, A. O., "Three-Dimensional Beltrami Flow in Turbomachinery with Strong Arbitrary Swirl," Ph.D. Thesis, Massachusetts Institute of Technology, Cambridge, Mass., June 1978.

[42] Oliver, D. A. and Sparis, P., "A Computational Study of Three-Dimensional Transonic Shear Flow in Turbomachine Cascades," AIAA Paper 71-83, Jan. 1971.

[43] Sparis, P., "A Computational Study of the Three-Dimensional Flow in a Single Stage Transonic Compressor," Ph.D. Thesis, Massachusetts Institute of Technology, Cambridge, Mass., Feb. 1974.

[44] Haymann-Haber, G., "A Computational Study of the Flow in a Transonic Axial Compressor Using an Inviscid Three-Dimensional Finite Difference Method," Massachusetts Institute of Technology, Gas Turbine and Plasmadynamics Rept. 145, May 1979.

[45] Thompkins, W. T., Jr., personal communication, Oct. 1979.

[46] Epstein, A. H., personal communication, Oct. 1979.

[47] Weyer, H. B., "Compressor Design and Experimental Results," *Through Flow Calculations in Axial Turbomachinery*, AGARD Conference Proceedings, 195, May 1976.

[48] Wennerstrom, A, J., Law, C. H., Buzzell, W. A., and Derose, R. D., "Investigation of a 1500 ft./sec. Transonic High-Through-Flow, Single Stage Axial Flow Compressor with Low Hub/Tip Ratio," AFAPL-TR-76-92, Oct. 1976.

[49] Bilwakesh, K. R., "Evaluation of Range and Distortion Tolerance for High Mach Number Transonic Fan Stages," Vol. II, NASA CR-72787, Jan. 1971.

[50] Urasek, D. C., Gorrell, W. T., and Cunnan, W. S., "Performance of Two Stage Fan Having Low Aspect Ratio, First Stage Rotor Blading," NASA Tech. Paper 1493, Aug. 1979.